Revista Mexicana de Astronomía y Astrofísica, **50**, 15–22 (2014)

uvby − *β* PHOTOELECTRIC PHOTOMETRY AND MEMBERSHIP DETERMINATION OF THE OPEN CLUSTER NGC 2353[1]

J. Segura,[2] A. Juárez,[3] and J. H. Peña[4]

Received 2012 December 6; accepted 2013 October 7

RESUMEN

A partir de fotometría fotoeléctrica *uvby* − *β* del cúmulo abierto NGC 2353 (55 estrellas) realizamos la determinación de distancias y, por ende, la pertenencia de las estrellas al cúmulo. Asimismo, se determinaron la edad y el enrojecimiento de éste.

ABSTRACT

From *uvby* − *β* photoelectric photometry of the open cluster NGC 2353 (55 stars) we were able to determine membership of the stars to the cluster and fix its age and reddening.

Key Words: open cluster and associations: individual (NGC 2353) — techniques: photometric

1. MOTIVATION

As a continuation of a study of open clusters, we present an analysis of membership in the open cluster NGC 2353 through the determination of the physical parameters of member stars. These can be determined from *uvby* − *β* photometry and the parameters predicted from the theoretical models (Lester, Gray, & Kurucz 1986, hereinafter LGK86). Some stars with *uvby* − *β* photometry were compiled by WEBDA[5]: eleven stars reported by Eggen (1978) and one star by several authors (Crawford, Barnes, & Golson 1971; Grønbech & Olsen 1976; Stetson 1991; Kaltcheva & Olsen 1999; Kaltcheva, Olsen, & Clausen 1999). See WEBDA for a detailed compilation. In view of this and of the instrumentation available, NGC 2353 was chosen because there are very few previous *uvby* − *β* data available. According to WEBDA NGC 2353 is at 1119 pc, its reddening is small (0.072 mag) and its distance modulus is 10.47; it has a log age of 7.974 and no metallicity is reported.

Open clusters are exceedingly important in many aspects of astronomical development, for example, as galactic tracers, to study blue stragglers, in studies of spectroscopic binaries, of variable stars, etc. There are very few studies devoted to the acquisition of new data for NGC 2353. One of the most recent works is that of Lim et al. (2011) who, through *UBVI* CCD photometry of the stars in the cluster (up to V=20 mag) determined the reddening and distance to the cluster to be $E(B-V)= 0.10 \pm 0.02$ mag and 1.17 ± 0.04 kpc, respectively. The age they determined is log (age) = 8.1 ± 0.1 yr, older than was found in previous studies. They obtained the luminosity function and initial mass function of the probable cluster members. Some other photometric studies were previously done by Hoag et al. (1961) and Fitzgerald, Harris, & Reed (1990). A summary is presented in WEBDA.

2. OBSERVATIONS

These were all performed at the Observatorio Astronómico Nacional, Mexico. The 1.5 m telescope to which a spectrophotometer was attached was utilized at all times. The observations were carried out in two seasons, in 2002 and 2003. The first observing season was from February 4 to February 11 and that of 2003, from January 9 to January 14. The ID charts utilized were those of WEBDA, selected for a limiting magnitude of around 13 mag, which is the reasonably reachable limit given by the telescope-spectrophotometer system. The nomenclature we followed is that of WEBDA and is denoted by a pre-

[1]Based on observations collected at the San Pedro Mártir Observatory, Mexico.

[2]Facultad de Ciencias Físico-Matemáticas, Universidad Autónoma de Coahuila, Mexico.

[3]Universidad Autónoma de la Ciudad de México, Mexico.

[4]Instituto de Astronomía, Universidad Nacional Autónoma de México, Mexico.

[5]`http://webda.physics.muni.cz/`.

TABLE 1

TRANSFORMATION COEFFICIENTS OBTAINED FOR THE OBSERVED SEASONS

Season	B	D	F	J	H	I	L
2002 and 2003	0.069	1.012	1.111	0.025	1.004	0.035	−1.333
σ	0.086	0.034	0.031	0.085	0.050	0.076	0.074

fix W. We measured 26 stars in the 2002 season and 49 stars in 2003.

2.1. *Data acquisition*

During all nights the following procedure was utilized: each measurement consisted of at least five ten-second integrations of each star and one ten-second integration of the sky for the *uvby* filters and the narrow and wide filters that define Hβ. Individual uncertainties were determined by calculating the standard deviations of the fluxes in each filter for each star. The percent error in each measurement is, of course, a function of both the spectral type and the brightness of each star, but the targets were observed long enough to secure sufficient photons to get a S/N ratio of accuracy of $N/\sqrt{(N)}$ of 0.01 mag in all cases.

2.2. *Data reduction*

The reduction procedure was done with the numerical package NABAPHOT (Arellano-Ferro & Parrao 1988) which reduces the data into a standard system. A series of standard stars was also observed on each night to transform the data into the standard system. The chosen standard system was that defined by the standard values of Olsen (1983) although some bright standard stars were taken from the Astronomical Almanac for the year 2003 (2001).

The transformation equations are those defined by Crawford & Barnes (1970) and by Crawford & Mander (1966). In these equations the coefficients D, F, H and L are the slope coefficients for $(b-y)$, m_1, c_1 and β, respectively. The coefficients B, J and I are the color terms of V, m_1, and c_1. However, in the 2002 season the range coverage of the standard stars that define m_1 was not ample enough to accurately determine this index. Hence, the coefficients, both slope and color coefficients for both seasons, were determined for each night and averaged. The average transformation coefficients for both seasons are listed in Table 1 along with their standard deviations, although shown for m_1 are those of the 2003 season only. Errors of the season were evaluated by means of the standard deviations of all values. These uncertainties were calculated through the differences in magnitude and colors, for (V, $b-y$, m_1, c_1 and β) as (0.074, 0.018, 0.012, 0.035, 0.012), respectively which provide a numerical evaluation of our uncertainties.

Emphasis is made on the large range of the standard stars in the magnitude and color values combined for both seasons: V:(5.8, 9.3); $(b-y)$:(-0.07, 0.66); m_1:(0.07, 0.72); c_1:(0.02, 1.91) and β:(2.53, 2.89).

Table 2 lists the photometric values of the observed cluster stars. For this list, the $uvby-\beta$ photometric values reported by WEBDA have been included to have a complete data set. Those that were observed only by us are of two kinds: those that have more than one measurement and have been averaged within our photometric measurements and those that were observed only once. In this table, Column 1 reports the ID of the stars as listed by WEBDA. The ID is reported in four different ways: (i) those within brackets $\langle$X$\rangle$ are mean values of the stars observed in the two seasons. (ii) Some were observed only once and the ID numbers do not have any special characteristics. (iii) Ten were observed both by us and previous studies and have values listed in WEBDA; they were averaged and are denoted by $[X]$ and, finally, (iv) only one star W04 was included that was observed previously and reported by WEBDA. It is marked with an asterisk. Columns 2 to 6 list the Strömgren values V, $(b-y)$, m_1, c_1, and Hβ, respectively; immediately below the averaged values the standard deviations are presented. Subsequent columns from 7 to 9 list the unreddened indexes $[m_1]$, $[c_1]$ and [u-b] derived from the observations. Column 10 lists the spectral types reported from the literature and the last column the reported spectral types inferred from the Strömgren photometry.

3. COMPARISON WITH OTHER PHOTOMETRIES

A comparison of our values with the UBV and $uvby-\beta$ photometry available in the literature was carried out to verify the goodness of our data. From the compilation of WEBDA the intersection of both sets UBV and our $uvby-\beta$ photometry is constituted of fifty-three points if we do not consider

TABLE 2

$uvby-\beta$ PHOTOELECTRIC PHOTOMETRY OF THE STARS IN THE DIRECTION OF THE OPEN CLUSTER NGC 2353

WEBDA	V	$b-y$	m_1	c_1	Hβ	$[m_1]$	$[c_1]$	$[u-b]$	Spectral Classification	
									Spectroscopic	Photometric
[1]	6.027	−0.028	−0.040	−0.080	2.578	−0.049	−0.074	−0.056		B5I
	0.010	0.021	0.120	0.031	0.010					
[2]	9.174	0.035	0.010	0.753	2.696	0.021	0.746	−0.663		AI
	0.009	0.021	0.092	0.018	0.051					
[3]	9.443	0.593	0.324	0.398	2.714	0.514	0.279	1.436		K0
	0.011	0.004	0.044	0.081						
4*	9.88	−0.075	0.250	0.700	2.807	0.226	0.715	−0.350	B9IIIp	A8V
7	10.940	0.345	−0.098	0.506	2.651	0.012	0.437	0.462	B9V	B9V
9	12.099	0.051	0.033	0.984	2.829	0.049	0.974	1.072		AI
13	13.515	0.330	−0.014	0.935	3.059	0.092	0.869	1.052		AI
[16]	9.391	0.043	0.026	0.725	2.646	0.040	0.716	−0.587	B8III-IV	AI
	0.013	0.010	0.077	0.006	0.081					
[17]	9.828	−0.008	050	0.614	2.726	0.047	0.616	−0.530	B8VN	AI
	0.017	0.018	0.093	0.012	0.009					
⟨18⟩	10.115	0.689	0.435	0.308	2.522	0.655	0.170	1.481		F2I
	0.040	0.014	0.018	0.047	0.044					
[19]	10.550	0.055	0.059	0.706	2.757	0.077	0.695	−0.7478	B8V	AI
	0.015	0.008	0.086	0.022	0.035					
[20]	10.902	0.026	0.054	0.634	2.712	0.062	0.589	−0.474	B8IV	AI
	0.026	0.041	0.065	0.065	0.029					
22	11.462	0.279	0.042	0.473	2.597	0.131	0.417	0.680	F2IV	B6
[24]	11.502	0.035	0.085	0.942	2.814	0.096	0.935	−0.702	B9.5V	B8
	0.025	0.008	0.092	0.005	0.087					
[25]	11.459	0.022	0.076	0.950	2.749	0.083	0.946	−0.754		AI
	0.027	0.025	0.076	0.007	0.094					
26	11.765	0.095	0.083	0.966	2.666	0.113	0.947	1.174		A9
⟨27⟩	11.618	0.073	0.014	1.024	2.819	0.037	1.009	1.084	B9V	AI
	0.027	0.024	0.003	0.082	0.055					
28	11.760	0.623	0.248	0.482	2.622	0.447	0.357	1.252		K0V
30	11.883	0.078	−0.023	0.852	2.628	0.002	0.836	0.840		AI
⟨31⟩	11.894	0.097	0.067	0.981	2.869	0.097	0.961	1.156		AI
	0.057	0.029	0.008	0.052	0.076					
⟨33⟩	11.900	0.022	0.069	0.987	2.861	0.076	0.982	1.133		AI
	0.004	0.027	0.008	0.110	0.036					
35	12.148	0.361	0.000	0.326	2.649	0.116	0.254	0.485		B2
⟨36⟩	12.313	0.078	0.080	1.019	2.825	0.104	1.004	1.212		AI
	0.023	0.052	0.026	0.117	0.015					
37	12.284	0.170	0.117	1.040	2.831	0.171	1.006	1.349		A0
38	12.322	0.096	0.136	1.015	2.914	0.167	0.996	1.329	A5.5V	A0
40	12.305	0.134	0.060	1.061	2.891	0.103	1.034	1.240		AI
41	12.438	0.092	0.113	0.857	2.742	0.142	0.839	1.123		B9V
42	12.539	0.149	0.069	1.073	2.904	0.117	1.043	1.277	A3V	AI
44	12.515	0.278	0.002	1.038	2.867	0.091	0.982	1.164		AI
45	12.468	0.144	0.060	1.073	2.902	0.106	1.044	1.256		AI
46	12.548	0.483	0.135	0.364	2.658	0.290	0.267	0.847		G0V
47	12.544	0.153	0.078	1.018	2.844	0.127	0.987	1.241		B9V
49	12.676	0.265	0.127	0.704	2.791	0.212	0.651	1.075		A9
⟨50⟩	12.661	0.292	−0.114	0.720	2.704	−0.021	0.661	0.620		AI
	0.004	0.009	0.175	0.021	0.049					
⟨53⟩	12.705	0.142	0.092	0.955	2.759	0.137	0.927	1.201	A3V	B9V
	0.054	0.150	0.165	0.171	0.016					
55	12.905	0.161	0.114	1.040	2.866	0.166	1.008	1.339		A0
57	12.969	0.365	0.075	0.485	2.647	0.192	0.412	0.796		F2
58	12.895	0.391	−0.015	0.460	2.687	0.110	0.382	0.602		B5V
60	13.001	0.222	0.074	0.954	2.840	0.145	0.910	1.200	A4V	B9V
61	13.049	0.236	0.051	0.935	2.864	0.127	0.888	1.141		B9V
64	13.220	0.286	0.047	1.007	2.771	0.139	0.950	1.227		B9V
65	13.153	0.245	0.054	0.823	2.770	0.132	0.774	1.039		B9V
69	13.299	0.157	0.145	0.839	2.848	0.195	0.808	1.198		A6
75	13.338	0.239	0.104	0.913	2.701	0.180	0.865	1.226		A2V
82	13.486	0.396	−0.030	0.507	2.730	0.097	0.428	0.621		B5V

TABLE 2 (CONTINUED)

WEBDA	V	$b-y$	m_1	c_1	Hβ	$[m_1]$	$[c_1]$	$[u-b]$	Spectral Classification	
									Spectroscopic	Photometric
84	13.643	0.347	−0.067	0.544	2.557	0.044	0.475	0.563		AI
[135]	8.820	0.025	0.021	0.396	2.595	0.029	0.391	−0.304	B5III	AI
	0.015	0.008	0.084	0.001	0.081					
136	11.682	0.029	0.034	0.996	2.675	0.043	0.990	1.077		AI
⟨137⟩	10.323	0.056	0.008	0.817	2.708	0.025	0.806	0.857		AI
	0.016	0.013	0.036	0.042	0.116					
138	13.109	0.351	−0.015	0.333	2.622	0.097	0.263	0.457		B2V
1141	12.966	0.423	0.018	0.624	2.747	0.153	0.539	0.846		B
⟨1148⟩	10.266	0.401	0.076	0.444	2.601	0.204	0.363	0.772		F5
	0.030	0.027	0.000	0.101	0.040					
1183	11.848	0.434	0.123	0.476	2.629	0.262	0.389	0.913		F9V
1184	12.115	0.060	0.104	1.040	2.934	0.123	1.028	1.274		A0V
⟨1⟩5022	12.166	0.118	0.039	0.949	2.806	0.077	0.925	1.079		AI
	0.076	0.038	0.040	0.119	0.068					
1181	11.900	0.047	0.073	1.014	2.892	0.088	1.005	1.181		AI
139+126	12.543	0.116	0.108	1.052	2.884	0.145	1.029	1.319		A0V

those values for which WEBDA assigns a V magnitude of 14 for the faint stars (only three stars). A direct comparison of the magnitudes gives a good agreement of $V_{\rm pp} = 0.068 + 0.993 \times V_{\rm WEBDA}$. Four points were discarded: stars W136, a bright star, and three fainter stars, W1141, W1148 and W139. The goodness of the fit is evaluated through a standard deviation of 0.060 and a correlation coefficient of 0.999. The magnitude range is between 6.0 mag to 13.7 mag. With respect to the color indexes $B-V$ and $(b-y)$, they are related by the equation $(b-y)$=0.028+0.587*$(B-V)$ with a standard deviation of 0.053 and a correlation coefficient of 0.94. Some points were discarded: W136 and W139, both of which were also discarded in the magnitude relation. We also compared the color index $U-B$ vs. $[u-b]$. As can be expected, this comparison is not as accurate as the previous ones. Two parallel branches appear in the $U-B$. The linear equation that relates both sets is $[u-b]$=0.932+1.019*$(U-B)$ with a standard deviation of 0.212 and a correlation coefficient of 0.783 for a sample of 53 entries.

With respect to the previous $uvby-\beta$ photometry constituted of a sample of eleven stars, an intersection set is constituted of ten stars, although W03 has no Hβ measurements reported. The agreement between both sets is adequate and is given by the good correlation coefficients for the linear fits: comparison of the magnitudes gives a good agreement of $V_{\rm pp} = 0.020 + 0.996 * V_{\rm WEBDA}$. The goodness of the fit is evaluated through a standard deviation of 0.024 and a correlation coefficient of 0.999 for the V magnitude. For the $(b-y)$ color comparison, we get $(b-y)_{\rm pp} = -0.019 + 1.028 * (b-y)_{\rm WEBDA}$, with a standard deviation of 0.024 and a correlation coefficient of 0.992. The m_1 index comparison gives $m_{1,\rm pp} = -0.148 + 1.246 * m_{1,\rm WEBDA}$, a standard deviation of 0.020 and a correlation coefficient of 0.985. The c_1 index comparison gives $c_{1,\rm pp} = 0.001 + 0.977 * c_{1,\rm WEBDA}$, a standard deviation of 0.054 and a correlation coefficient of 0.986. The Hβ index comparison is not as good as the color indexes; the comparison gives H$\beta_{\rm pp} = 0.681 + 0.724$*H$\beta_{\rm WEBDA}$ with a standard deviation of 0.050 and a correlation coefficient of 0.800. Two of the stars with largest differences are faint stars, of magnitudes 11.52 (W24) and 11.44 (W25).

Hence, given the large number of measured stars in good agreement with the reported photometry, we consider that our measurements are accurate and reliable. Hence, our analysis should be meaningful.

4. METHODOLOGY

In order to determine the physical characteristics of the stars in the cluster this procedure was followed:

The evaluation of the reddening was done by first establishing, as was stated above, to which spectral class the stars belong: early (B and early A) or late (late A and F stars) types; later class stars (G or later) were not considered in the analysis since no reddening determination calibration has yet been developed for them. In order to determine the spectral type of each star, the location of the stars in the $[m_1]-[c_1]$ diagram was employed as a primary criterion.

The application of the calibrations for each type (Shobbrook 1984, for O and early A type; Nissen 1988, for late A and F stars, respectively) allowed us to determine the reddening for each star, and hence its unreddened indexes, as well as its distance. (See

TABLE 3

REDDENING AND UNRREDDENED PARAMETERS OF THE MEASURED STARS IN THE DIRECTION OF THE OPEN CLUSTER NGC 2353

ID	$E(b-y)$	$(b-y)_0$	m_0	c_0	Hβ	V_0	M_V	DM	DST	[Fe/H]	Membership
1148	0.080	0.321	0.100	0.428	2.601	9.9	2.4	7.5	318	−0.93	NM
1183	0.113	0.321	0.157	0.453	2.629	11.4	2.5	8.9	597	−0.23	NM
49	0.104	0.161	0.158	0.683	2.791	12.2	3.3	8.9	608		NM
57	0.085	0.280	0.101	0.468	2.647	12.6	2.7	10.0	978	−0.79	M
69	0.056	0.101	0.162	0.828	2.848	13.1	2.8	10.2	1112		M
17	0.028	−0.049	−0.008	0.617	2.732	9.7	−0.5	10.2	1116		M
1184	0.065	−0.005	0.124	1.028	2.934	11.8	1.6	10.3	1142		M
44	0.295	−0.017	0.090	0.982	2.867	11.3	1.0	10.3	1147		M
31	0.118	−0.021	0.102	0.959	2.869	11.4	1.0	10.4	1202		M
38	0.110	−0.014	0.169	0.994	2.914	11.9	1.4	10.5	1235		M
1181	0.059	−0.012	0.091	1.003	2.892	11.7	1.2	10.5	1236		M
1	0.108	−0.121	−0.093	−0.078	2.571	5.6	−5.0	10.5	1270		M
40	0.137	−0.003	0.101	1.035	2.891	11.7	1.2	10.6	1292		M
45	0.144	0.000	0.103	1.046	2.902	11.9	1.3	10.6	1314		M
42	0.149	0.000	0.114	1.045	2.904	11.9	1.3	10.6	1331		M
19	0.092	−0.043	0.026	0.703	2.732	10.1	−0.6	10.8	1426		M
33	0.039	−0.017	0.081	0.980	2.861	11.7	0.9	10.8	1474		M
24	0.000	0.169	0.020	0.938	2.752	11.5	0.6	10.9	1485		M
27	0.084	−0.011	0.039	1.008	2.819	11.3	0.4	10.9	1514		M
61	0.267	−0.031	0.131	0.884	2.864	11.9	1.0	10.9	1532		M
139	0.121	−0.005	0.144	1.029	2.884	12.0	1.1	10.9	1535		M
37	0.181	−0.011	0.171	1.006	2.831	11.5	0.5	11.0	1575		M
47	0.169	−0.016	0.129	0.986	2.844	11.8	0.7	11.1	1678		M
1141	0.479	−0.056	0.162	0.533	2.747	10.9	−0.3	11.2	1726		M
137	0.094	−0.038	0.036	0.799	2.708	9.9	−1.3	11.2	1734		M
60	0.251	−0.029	0.149	0.906	2.840	11.9	0.7	11.2	1749		M
7	0.412	−0.067	0.026	0.428	2.651	9.2	−2.1	11.2	1765		M
55	0.172	−0.011	0.166	1.007	2.866	12.2	0.9	11.2	1773		M
5022	0.145	−0.027	0.082	0.921	2.806	11.5	0.3	11.3	1791		M
9	0.070	−0.019	0.054	0.971	2.829	11.8	0.5	11.3	1796		M
2	0.062	−0.042	−0.036	0.728	2.660	8.9	−2.5	11.4	1880		M
36	0.090	−0.012	0.107	1.002	2.825	11.9	0.4	11.5	1978		M
20	0.049	−0.052	0.023	0.579	2.691	10.7	−1.3	12.0	2464		NM
65	0.285	−0.040	0.139	0.769	2.770	11.9	−0.1	12.0	2523		NM
82	0.464	−0.068	0.109	0.419	2.730	11.5	−0.5	12.0	2534		NM
58	0.465	−0.074	0.124	0.372	2.687	10.9	−1.2	12.1	2643		NM
64	0.309	−0.023	0.140	0.948	2.771	11.9	−0.3	12.2	2723		NM
35	0.451	−0.090	0.135	0.240	2.649	10.2	−2.0	12.2	2767		NM
50	0.338	−0.046	−0.013	0.656	2.704	11.2	−1.1	12.3	2910		NM
53	0.169	−0.027	0.143	0.923	2.759	12.0	−0.5	12.4	3067		NM
41	0.128	−0.036	0.151	0.833	2.742	11.9	−0.6	12.5	3181		NM
25	0.027	−0.023	0.030	0.950	2.682	11.4	−2.4	13.8	5614		NM
75	0.272	−0.033	0.186	0.861	2.701	12.2	−1.6	13.8	5627		NM
138	0.440	−0.089	0.117	0.249	2.622	11.2	−2.7	13.9	6131		NM
22	0.349	−0.070	0.147	0.407	2.597	10.0	−4.2	14.2	6881		NM
136	0.045	−0.016	0.047	0.988	2.675	11.5	−2.8	14.2	7032		NM
26	0.000	0.233	0.083	0.966	2.666	11.8	−2.6	14.4	7517	−1.00	NM
16	0.079	−0.043	−0.005	0.714	2.589	9.0	−6.5	15.5	12823		NM
30	0.114	−0.036	0.011	0.830	2.628	11.4	−4.3	15.7	13470		NM

Peña & Peniche 1994 for a detailed description of the method).

5. RESULTS

In Table 2 the photometrically determined spectral class has been indicated. The determined spectral types compiled by WEBDA are also presented.

Of the 55 measured stars, only two were fixed as very late type stars, none of which were previously assigned a spectral type (W03 and W28). Nine (W4, W18, W26, W46, W49, W57, W69, W1148, and W1183) are of spectral types later than A5 and for which the prescription of Nissen (1988) is applicable. The remaining stars, whose spectral types we assigned, are all early type stars. Most of them were not previously spectroscopically classified and for those which had been calibrated, the majority agree with the previous spectral classification. We call at-

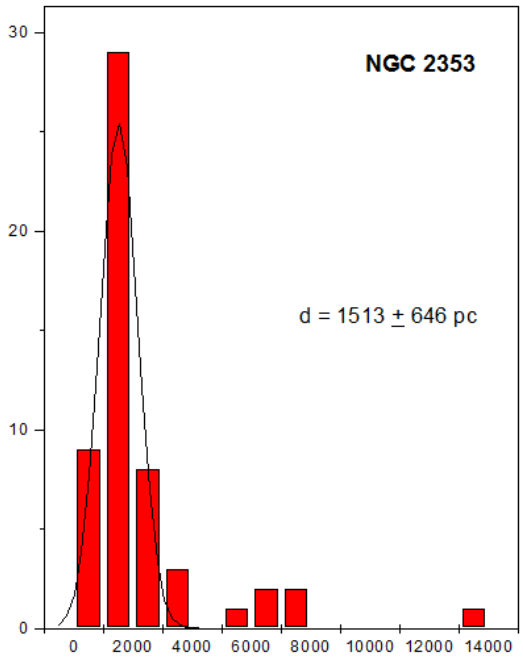

Fig. 1. Histogram of the distances found for the stars in the direction of the cluster. The continuous line is a Gaussian fit to the distribution. Mean value and standard deviation are presented.

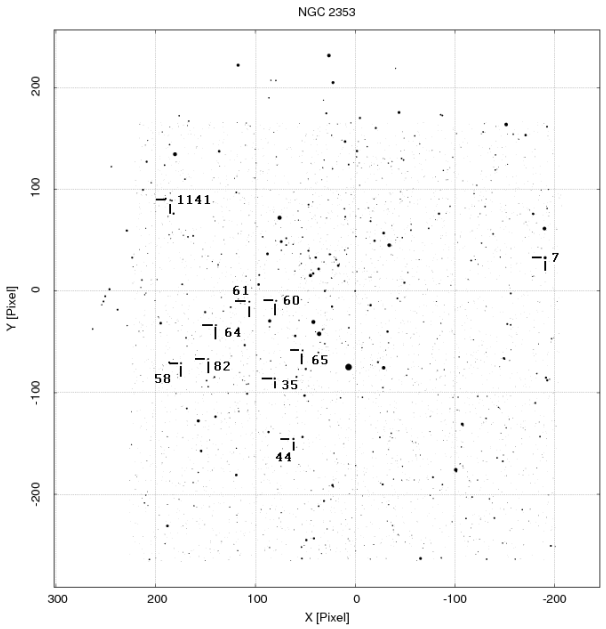

Fig. 2. Identification chart of stars in the direction of NGC 2353 with large reddening values.

tention to the good agreement between the types reached by two different approaches. Quite a few belong to what Golay (1974) describes as Region 1 in his Figure 123 as A type stars of luminosity class I. There is one discordant classification: star W22.

Once the stars were spectrocopicaly classified, we were able to apply the numerical calibrations described in the previous section. The application of the above mentioned numerical packages gave the results listed in Table 3 in which the ID, reddening, unreddened indexes, absolute magnitude, distance modulus DM and distance, are listed. A brief discussion of the cluster is presented.

6. ANALYSIS

A visualization of the distance distribution for all stars can be done through statistics. From the reported distance values, listed in Table 3 and shown schematically in Figure 1, we can establish that NGC 2353 has a distinctive accumulation of stars. As can be seen in Figure 1, the majority of the stars lie in a well defined peak which throws light on the distribution of the distance for the members to the cluster. There are few, six, whose distances are clearly beyond the cluster limits. To discriminate and assign membership probabilities we calculated a Gaussian fit which provides us with a mean distance value as well as a standard deviation for the fit. We define member stars those whose distances are one sigma from the mean value. The Gaussian fit gave the following values: The cluster is located at a distance modulus (DM) of 11.05 ± 1.91 or, in the distance histogram, at a distance of 1513 ± 645 pc. The sample of stars we have measured, although not huge, is significant: more than fifty measured stars of which thirty were found to be members of NGC 2353. In this table, listed in increasing distance, Column 1 presents the ID; Column 2 the reddening $E(b-y)$ and Columns 3 to 5 the unrreddened indexes. Hβ is presented in Column 6. V_0 and M_V are presented in Columns 7 and 8. The distance modulus DM and the distance in the subsequent columns. The last column presents membership. Those stars considered as members are denoted by M; NM stands for those out of the cluster limits. Star W01 has been listed in WEBDA as a member star from proper motion studies. Star W02, which has a low value of probability was determined to be a member in our study.

Once we have determined the member stars, some properties of the cluster can be deduced. For example, average distance for the member stars is 1443 ± 664 pc. Average reddening has values of 0.14±0.11 mag, but there are some stars which have an anomalously large reddening. Without them the average reddening is of 0.10 ± 0.05 mag. In order to find out why this anomaly exists we constructed a

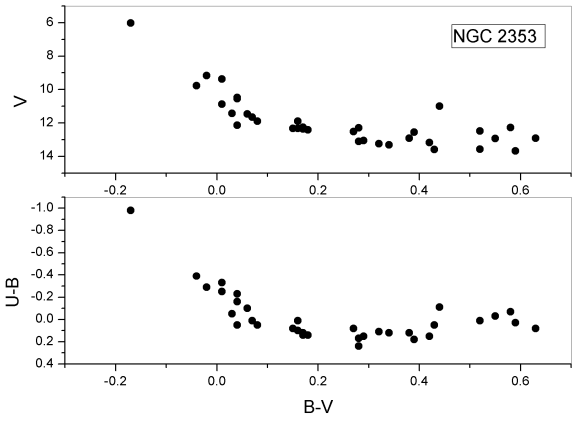

Fig. 3. $U-B$ vs. $B-V$ (lower) and V vs. $B-V$ (upper) for the member stars of NGC 2353.

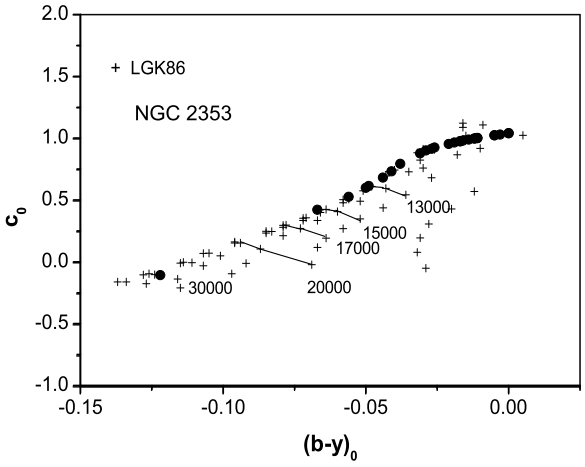

Fig. 4. Location of the unreddened points (black dots) of the member stars to NGC 2353 in the LGK86 grids.

V, $B-V$ diagram for the stars with high reddening (not only member stars) and located these stars in WEBDA's ID chart (Figure 2). It is remarkable that most of them lie in a well-defined central region, suggesting a well-located dark cloud between the cluster and the Sun.

Once we determined the cluster members, we calculated their values in UBV photometry as reported in WEBDA. Plots of the color-color and color-magnitude diagrams were constructed. Figure 3 represents these diagrams: $U-B$ vs. $B-V$ and V vs. $B-V$ for the member stars. We call attention to star W1 which is a blue straggler, already pointed out as such in WEBDA's list.

WEBDA does not report metallicity for this cluster. What we did to determine it in order to be able to choose a model, was to consider clusters in the direction of NGC 2353 for which metallicity has been determined: NGC 2355 (-0.07) and NGC 2360 (-0.14 ± 0.08) and since their metallicities (in parentheses) are not far from a solar composition, we assumed this metallicity and utilized the $(b-y)_0$ vs. c_0 diagrams which allow the determination of the temperatures with an accuracy of a few hundreds of degrees (Figure 4). The hottest star, W1, has a T_e of 30,000 K; the second hottest star, W07, 15,000 K and the third, W1141, 14,000 K. Since the membership has been established, age is determined after calculating the effective temperature through the calibrations of Meynet, Mermilliod, & Maeder (1993) for open clusters; log age is found from the relation log age $= -3.499\ \log T_e + 22.476$ valid in the range log T_e within the limits [4.25, 4.56] and log age $= -3.611$ log $T_e + 22.956$ in the range log T_e within the limits $[3.98, 4.25]$. For the hottest star, W1, in NGC 2353 a log age of 6.81 (2.2×10^8 yr) is obtained, but we must keep in mind that this is a blue straggler and hence it was not considered for the age determination. For the second star W07, a log age of 7.9 (9.0×10^8 yr) is determined.

7. DISCUSSION

New $uvby-\beta$ photoelectric photometry has been acquired and is presented for the brightest stars in the direction of the open cluster NGC 2353. Most of the observed stars in the field, were determined to be early type stars, either B or A. Using the calibrations to determine reddening and distance to these stars, the distance to the cluster has been obtained. Unreddened indexes in the LGK86 grids allowed us to determine the effective temperature of the hottest stars.

A brief summary of the results for the cluster is presented. Table 4 lists the previous and newly determined characteristics of the cluster.

Considering only the classical UBV photometry compiled for this cluster, very little can be deduced about its properties. Although a clear distinction relative to membership from the color-color diagram $B-V$ vs. $U-B$ can be drawn; the same conclusion is not reached from its HR diagram. From our results we have determined 26 stars to be at the same distance limits. Since they are the brightest, the conclusion on the age, which agrees with the previously determined value, is correct. We have found that the cluster is farther than previously assumed and its extinction is slightly smaller than previously determined. In reference to the membership, the goodness of our method has been tested (as in the case of the open cluster Alpha Per; Peña & Sareyan 2006)

TABLE 4

SUMMARY OF CHARACTERISTICS FOR THE NGC 2353 CLUSTER

Property	WEBDA	Lim et al.	PP
Right Ascension	07 14 30		
Declination	−10 16 00		
Galactic longitude	224.685		
Galactic latitude	0.384		
Distance [pc]	1119	1170 ± 400	1513 ± 646
Reddening [mag] $E(B-V)$	0.072	0.10 ± 0.02	0.02 ± 0.01
Reddening [mag] $E(b-y)$			0.15 ± 0.11
Distance modulus [mag]	10.47		11.0 ± 1.2
Log age	7.974	8.1 ± 0.1	7.86

against several sources in which proper motion studies are considered, as well as results from the Hipparcos and Tycho databases. From these tests, we have found an agreement between our data and those of the literature. For NGC 2353 the results found are consistent with WEBDA's membership. Hence, we feel that our results throw new light on membership in this cluster as well as its physical parameters.

8. CONCLUSIONS

We have presented $uvby-\beta$ photoelectric photometry of the open cluster NGC 2353. From it we were able to determine both the spectral types and membership of the stars to the cluster and its age and distance.

We would like to thank the staff of the OAN and L. Parrao for their assistance in securing the observations. This work was partially supported by PAPIIT IN104612 and PAPIME PE103112. AJ and JS thank the IA-UNAM for the opportunity to carry out the observations. This work will be presented as part of the MSc degree requirements at the Instituto de Astronomía. Typing and proofreading were done by J. Orta, and J. Miller, respectively. C. Guzmán, F. Ruiz and A. Diaz assisted us in computing. This research has made use of the Simbad databases operated at CDS, Strasbourg, France and NASA ADS Astronomy Query Form.

REFERENCES

Arellano-Ferro, A., & Parrao, L. 1988, Reporte Técnico 57 (Mexico: Instituto de Astronomía, Univ. Nacional Autónoma de México)
Crawford, D. L., & Barnes, J. V. 1970, AJ, 75, 978
Crawford, D. L., Barnes, J. V., & Golson, J. C. 1971, AJ, 76, 621
Crawford, D. L., & Mander, J. 1966, AJ, 71, 114
Eggen, O. J. 1978, PASP, 90, 436
Fitzgerald, M. P., Harris, G. L., & Reed, B. C. 1990, PASP, 102, 865
Golay, M. 1974, Introduction to Astronomical Photometry (Dordrecht: Reidel)
Grønbech, B., & Olsen, E. H. 1976, A&AS, 25, 213
Hoag, A. A., et al. 1961, Pub. US Naval Obs., 17, 344
Kaltcheva, N. T., & Olsen, E. H. 1999, A&A, 352, 600
Kaltcheva, N. T., Olsen, E. H., & Clausen, J. V. 1999, A&A, 353, 605
Lester, J. B., Gray, R. O., & Kurucz, R. I. 1986, ApJS, 61, 509 (LGK86)
Lim, B., Sung, H., Karimov, R., & Ibrahimov, M. 2011, J. Korean Astron. Soc., 44, 39
Meynet, G., Mermilliod, J. C., & Maeder, A. 1993, A&AS, 98, 477
Nissen, P. 1988, A&A, 199, 146
Olsen, E. H. 1983, A&AS, 54, 55
Peña, J. H., & Peniche, R. 1994, RevMexAA, 28, 139
Peña, J. H., & Sareyan, J. P. 2006, RevMexAA, 42, 179
Shobbrook, R. R. 1984, MNRAS, 211, 659
Stetson, P. B. 1991, AJ, 102, 589
U.S. Naval Observatory & Royal Greenwich Observatory 2001, The Astronomical Almanac for the year 2003 (Washington: USGPO; London: The Stationery Office)

A. Juárez: Instituto de Educación Media Superior José María Morelos y Pavón, Canal de Chalco esq. Piraña, Col. del Mar, C.P. 13270, México, D.F., Mexico (alfre_jv_iems@live.com.mx).
J. H. Peña: Instituto de Astronomía, Universidad Nacional Autónoma de México, Apdo. Postal 70-264, México, D.F. Mexico (jhpena@astro.unam.mx).
J. Segura: Facultad de Ciencias Físico-Matemáticas, Universidad Autónoma de Coahuila, C.P. 25280, Saltillo, Coahuila, Mexico (juan_segura@uadec.edu.mx).